PLASMA PHYSICS

H. GUERRIDA,[1] K. CHENINI,[2] M.T. MEFTAH,[1] S. DOUIS,[1] D.E. ZENKHRI,[3] K. ARIF [3]

[1] Faculty of Mathematics and Matter Sciences and LRPPS Laboratory, Kasdi Merbah University
  (30000 Ouargla, Algeria)
[2] Laboratoire MESTEL, Faculté des Sciences et de la Technologie, Université de Ghardaia
  (BP 455, Ghardaïa 47000, Algeria)
[3] LRPPS Laboratory, Kasdi Merbah University

IMPACT COLLISION OPERATOR FOR UNBOUNDED ELECTRONS IN A MAGNETIZED PLASMA MODEL

The shapes of spectral lines in plasmas contain information about plasma parameters and can be used as a diagnostic tool. We have obtained a theoretical expression involving a Meijer function for the plasma collision operator for electrons in the presence of an external magnetic field. We have used the semiclassical theory and the impact approximation which concern the interaction between the emitting systems (hydrogen-like ions in this study) and the plasma electrons. We have calculated the collision operator amplitude for some hydrogen-like ions such as Ar^{+17}, V^{+22}, Cr^{+23}, Fe^{+25}, and Ag^{+46} for high density intervals between $10^{18} \, cm^{-3}$ to $10^{26} \, cm^{-3}$ and at high temperatures between $10^6 \, K$ to $10^{10} \, K$ in a very strong magnetic field between 100 T to 10,000 T. We have applied our results to the Lyman-alpha line, and the comparison with experimental data and some theoretical results gives a good agreement.

K e y w o r d s: collision operator for electrons, external magnetic field, plasma spectroscopy.

1. Introduction

Magnetized plasmas are very important systems found in stars and thermonuclear fusion. Therefore, it is interesting to study the phenomena taking place in these plasmas, especially the collision effects. Spectral line profiles and shifts are used to determine plasma parameters, in particular, in astrophysics, where the plasma spectroscopy is the most used diagnostic technique. Nowadays, the latter covers a wide range of electron densities from 10 particles (inter-

stellar space) to 10^{25} particles per cm³ (star interiors, inertial confinement fusion) and for temperatures between 10^5 K and 10^8 K. Furthermore, the spectral line profile gives the distribution of the intensity of the radiation emitted by a plasma around the central frequency. It is a representation of the emitting atom and its surrounding. The atom/or ion will respond to the multiple microscopic interactions which preceded or accompanied the emission by: a broadening, a shift of its components, or by the removal of a degeneracy. One part of the broadening of the line profile is caused by the collision of the free electron with the emitters (atoms/ions) [1].

The Stark effect is due to the action of the electric field on the energy levels of an atom or ion emitters. It is caused by the interaction between the electric microfield and the dipole of this emitter [2, 3]. A.A. General and Yu.O. Shpenik [4] studied a gas-discharge

plasma in water vapor to improve the power characteristics of the discharge plasma.

The presence of the electric microfield generated by the unbounded (free) electrons induces a coupling between the energy levels which can be presented in the formalism of isolated lines by a direct term ϕ_d and by the interference term ϕ_{int} [5, 6]. The best evaluations of the expressions of ϕ_d and ϕ_{int} were given in [7], so the calculation of the electronic collision operator has the interest for several researchers for a long time [8, 9]. In the recent work by Arif *et al.* [9], the collision operator was calculated in the relativistic case in high-temperature plasma. The relativistic effects related to the Lienard–Wiechert electric field, created by the free electron at the emitter ion, and a modification of the hyperbolic trajectory due to the dependence of the mass on the free electron velocity. The fine structure was considered in work [9], and the results were confronted to the theoretical and experimental data available in the literature therein.

In the framework of the dipolar approximation and the impact theory, the electronic collision operator can be calculated for an emitter ion with electric charge $(+Ze)$ perturbed by an unbounded (free) electrons.

The action of a magnetic field on the energy levels of atoms was studied by Zeeman in 1896 [10]. He observed a decomposition of each emission line of the atoms into several co-components: this is the Zeeman effect. This effect comes from the interaction of the magnetic field with the orbital magnetic moment due to the movement of the electron in its orbit, and also with the magnetic moment associated with the spin of this electron. This eliminates the degeneracy of the energy levels of the atoms or the ions, where the degeneracy removal depends on the intensity of the magnetic field. The presence of magnetic fields increases the complexity of line-shape calculations in plasmas. A magnetic field has three essential effects on Stark-broadened spectral lines: (i) partial polarization of the emitted light, (ii) additional splitting according to the value of the magnetic quantum number m, and (iii) bending the colliding charged-particle trajectories into a helical path around the magnetic lines of force [11]. The effect of a magnetic field on the line profiles via a modification of the trajectories of the unbounded electrons was widely studied. Under specific conditions,

the plasma at the edge of tokamaks has parameters similar to those of white-dwarf magnetic stellar atmospheres [12–14], suggesting that the same line patterns may be used.

Some white dwarfs have a magnetic field strong enough, so that the quadratic Zeeman effect becomes significant. The line profiles become asymmetric and present more components [15]. About 10 percent of white dwarfs are known to have a magnetic field strength of to 50,000 Gauss (5 Teslas), as indicated by spectroscopic observations and models [16,17]. An interpretation of the profiles of absorption lines requires the Zeeman effect be accounted in line broadening models, as done in tokamak edge plasma spectroscopy [18]. R. Brauer *et al.* simulated the Zeeman splitting of the 1,665 MHz OH line with the 3D radiative transfer (RT) extension ZRAD [19]. L. Godbert-Mouret *et al.* [20] modified a model for the description of the Stark broadening to include the effect of a uniform magnetic field. This model is a convenient framework for treating, in a non-perturbative approach, the simultaneously acting Zeeman and Stark effects, while retaining the effect of ion dynamics [20]. So, the effect of an external magnetic field is studied theoretically and experimentally by many researchers [11, 21] and [22]. O.O. Loginov *et al.* [23] gave an explanation of the origin and the nature of the spatio-temporal variations of the magnetic activity of the Sun; while S. Nasrin and M. Bose [24] studied the effect of two different temperatures in an auroral ionosphere.

S. Ferri *et al.* [11] presented a Stark–Zeeman spectral line-shape model and the associated numerical code for strongly magnetized plasmas. Recent studies of how the B-fields influence electron trajectories in hydrogen plasmas were performed in the context of magnetic fusion and white dwarfs ([13,14], [25,26]). It was shown that introducing helical trajectories reduces the characteristic duration of the perturbation to the order of the inverse of the Larmor frequency, i.e., $\tau \sim 2\pi/\omega \sim 2\pi m_e\, c/eB$, which results in the line-shape narrowing. Such results suggest a modification of the electron collision operator generally used to describe the electronic Stark effect in line-shape modeling.

In the classical path approximation, the trajectory of an electron near a neutral atom is a straight line, while, near an ion, the trajectory is a hyperbola. In the presence of a magnetic field, it can be proved that the trajectory is helical [27].

We have developed the expression for the electron collision operator in magnetic plasma ϕ_B, when the trajectory of electrons is changed by the magnetic field, and we have used the collision operator to test the broadening of spectral lines for some ions and made a comparison with other expressions with and without magnetic field to see the magnetic field effect.

This work is considered the first, because, through it, we try to study the collisions that also occur in the Sun and other stars, by accounting for the physical conditions (very strong magnetic field; very high temperature, and very high electronic densities).

The interest of our work is to give the new formula of the electronic collision operator in a haut and dense plasma in the presence of an external magnetic field. We are interested in hot and dense plasmas such as thermonuclear fusion plasmas and certain stars. We treat the hydrogen-like ions such as Ar^{+17}, V^{+22}, Cr^{+23}, Fe^{+25}, and Ag^{+46} for high density intervals between 10^{18} cm^{-3} to 10^{26} cm^{-3} and high temperatures between 10^6 K to 10^{10} K and in a very strong magnetic field between 100 T to 10 000 T. In our work, we will consider the following hypothesis: the Maxwellian velocity distribution is unaffected by the magnetic field, the impact parameter changes, when an external magnetic field is applied in a plasma, the shielding is also not affected, e.g., Debye screening. In principle, since the shielding is provided by the motion/rearrangement of plasma electrons and ions, any field that affects their motion will also affect the shielding. However, as discussed above, the normal Debye shielding is assumed [27].

This paper is organized in four sections. In the second section, we will compute the collision operator expression in the presence of a magnetic field. The third section is devoted to the discussion of the obtained results, and we present the spectral line with this novel expression of the collision operator obtained in Sec. 2, while the last section summarizes the results in the conclusion.

2. Collision Operator Amplitude

Our departure point is Eqs. (5)–(6) of [7]. We will consider the case of the absence of a fine structure. Then we have $\omega_1 = \omega_2 = 0$. Let us take the limit of integrals over the time to be t_- and t_+ [26, 27]. Under these considerations, we have to compute (a_0 is Bohr's radius) the two "components" of the collision operator amplitude (in unit Hz/cm^2)

$$\Phi_d = -\frac{2\pi N_e e^2}{3\hbar^2} \int\limits_0^\infty v f(\mathbf{v}) d\mathbf{v} \int\limits_{\rho_-}^{\rho_+} \rho \, d\rho \times$$

$$\times \int\limits_{t_-}^{t_+} dt_1 \int\limits_{t_-}^{t_1} dt_2 \boldsymbol{\varepsilon}(t_1)\boldsymbol{\varepsilon}(t_2), \tag{1}$$

$$\Phi_{\text{int}} = -\frac{2\pi N_e e^2}{3\hbar^2} \int\limits_0^\infty v f(\mathbf{v}) d\mathbf{v} \int\limits_{\rho_-}^{\rho_+} \rho \, d\rho \times$$

$$\times \int\limits_{t_-}^{t_+} dt_1 \int\limits_{t_-}^{t_+} dt_2 \boldsymbol{\varepsilon}(t_1)\boldsymbol{\varepsilon}(t_2). \tag{2}$$

It is clear from these two expressions that $\phi_{\text{int}} = 2\phi_d$. It is the reason to calculate $\phi_{\text{int}} = a_0^2 \, \Phi_{\text{int}}$ (in Hz, and a_0 is Bohr's radius), i.e.,

$$\phi_{\text{int}} = -\frac{2\pi N_e}{3} \left(\frac{\hbar}{m_e e}\right)^2 \int\limits_0^\infty v f(\mathbf{v}) d\mathbf{v} \int\limits_{\rho_-}^{\rho_+} \rho \, d\rho \times$$

$$\times \int\limits_{t_-}^{t_+} dt_1 \int\limits_{t_-}^{t_+} dt_2 \boldsymbol{\varepsilon}(t_1)\boldsymbol{\varepsilon}(t_2) \tag{3}$$

such that $\boldsymbol{\varepsilon}(t_i) = e\frac{\mathbf{u}_i}{r^2(t_i)}$ is the individual electric microfield created by the unbounded electron that rotates around the applied magnetic field B. We must now solve the movement equations for this electron and for the ion, both being subjected to the action of magnetic and electric microfields. The movement equations (in CGS units) are as follows:

$$m\frac{d\mathbf{v}}{dt} = \left[-Ze\boldsymbol{\varepsilon}(t) - e\frac{\mathbf{v} \times \mathbf{B}}{c}\right], \tag{4}$$

$$M\frac{d\mathbf{V}}{dt} = \left[Ze\boldsymbol{\varepsilon}(t) + Ze\frac{\mathbf{V} \times \mathbf{B}}{c}\right], \tag{5}$$

where Z is the net charge of the emitting ion ($Z = Z_a - 1$ for the hydrogen-like ion), and c is the speed of light in the vaccum. We will take it equal to one, and we will reconsider in the elaboration of the final results (tables and figures). As the ratio of the masses of an electron and the ion is very small ($m_e/m_i \ll 1$), the electron dynamics is more affected by the magnetic field, whereas the ion dynamics is more affected

by the electric microfield created by the electron. So, we have

$$m\frac{d\mathbf{v}}{dt} \simeq -e\mathbf{v} \times \mathbf{B}, \tag{6}$$

$$M\frac{d\mathbf{V}}{dt} \simeq Ze\boldsymbol{\varepsilon}(t). \tag{7}$$

Then

$$\boldsymbol{\varepsilon}(t_1)\,\boldsymbol{\varepsilon}(t_2) \equiv C(t_1, t_2) = \left(\frac{M}{Ze}\right)^2 \frac{d\mathbf{V}(t_1)}{dt_1}\frac{d\mathbf{V}(t_2)}{dt_2}. \tag{8}$$

By using the momentum conservation $\mathbf{P}_0$ of the system (ion-electron-magnetic field), we have

$$\mathbf{p} + e\mathbf{A} + \mathbf{P} - Ze\mathbf{A} = \mathbf{P}_0, \tag{9}$$

$$m\mathbf{v} + M\mathbf{V} + e\mathbf{A}(e) - Ze\mathbf{A}(i) = \mathbf{P}_0. \tag{10}$$

Calculating the time derivative of the last equation, we obtain

$$m\frac{d\mathbf{v}(t)}{dt} + M\frac{d\mathbf{V}(t)}{dt} + e\frac{d\mathbf{A}(e)}{dt} - Ze\frac{d\mathbf{A}(i)}{dt} = \mathbf{0}, \tag{11}$$

$$\frac{d\mathbf{V}(t)}{dt} = -\frac{m}{M}\frac{d\mathbf{v}(t)}{dt} - \frac{e}{M}\frac{d\mathbf{A}(e)}{dt} + \frac{Ze}{M}\frac{d\mathbf{A}(i)}{dt}. \tag{12}$$

By using the gauge

$$\mathbf{A}(e) = \frac{B}{2}\begin{pmatrix} -y \\ x \\ 0 \end{pmatrix}; \quad \mathbf{A}(i) = \frac{B}{2}\begin{pmatrix} -Y \\ X \\ 0 \end{pmatrix}, \tag{13}$$

we get

$$\frac{d\mathbf{V}(t)}{dt} = -\frac{m}{M}\frac{d\mathbf{v}(t)}{dt} - \frac{e}{M}\frac{B}{2}\begin{pmatrix} -v_y \\ v_x \\ 0 \end{pmatrix} + \\ + \frac{Ze}{M}\frac{B}{2}\begin{pmatrix} -V_y \\ V_x \\ 0 \end{pmatrix}. \tag{14}$$

By replacing (15) in Eq. (8), we find

$$C(t_1, t_2) = \left(\frac{M}{Ze}\right)^2 \frac{d\mathbf{V}(t_1)}{dt_1}\frac{d\mathbf{V}(t_2)}{dt_2} = \\ = \left(\frac{M}{Ze}\right)^2 \left[\frac{m}{M}\frac{d\mathbf{v}(t_1)}{dt_1} + \frac{e}{M}\frac{B}{2}\begin{pmatrix} -v_y(t_1) \\ v_x(t_1) \\ 0 \end{pmatrix} - \\ - \frac{Ze}{M}\frac{B}{2}\begin{pmatrix} -V_y(t_1) \\ V_x(t_1) \\ 0 \end{pmatrix}\right]\left[\frac{m}{M}\frac{d\mathbf{v}(t_2)}{dt_2} + \\ + \frac{e}{M}\frac{B}{2}\begin{pmatrix} -v_y(t_2) \\ v_x(t_2) \\ 0 \end{pmatrix} - \frac{Ze}{M}\frac{B}{2}\begin{pmatrix} -V_y(t_2) \\ V_x(t_2) \\ 0 \end{pmatrix}\right]. \tag{15}$$

Here, we can neglect the last two terms in the right brackets which are with Z factor. For the same reason on the difference of masses, we can approximatively write

$$C(t_1, t_2) = \left(\frac{m}{Ze}\right)^2 \frac{d\mathbf{v}(t_1)}{dt_1}\frac{d\mathbf{v}(t_2)}{dt_2} + \\ + \frac{B^2}{4Z^2}(v_y(t_1)v_y(t_2) + v_x(t_1)v_x(t_2)) + \frac{mB}{2eZ^2} \times \\ \times \left(\frac{d\mathbf{v}(t_1)}{dt_1}\begin{pmatrix} -v_y(t_2) \\ v_x(t_2) \\ 0 \end{pmatrix} + \frac{d\mathbf{v}(t_2)}{dt_2}\begin{pmatrix} -v_y(t_1) \\ v_x(t_1) \\ 0 \end{pmatrix}\right). \tag{16}$$

The movement equation for the electron allows us to write

$$m\frac{d\mathbf{v}}{dt} \simeq -e\mathbf{v} \times \mathbf{B} = -e\begin{pmatrix} v_x(t) \\ v_y(t) \\ 0 \end{pmatrix} \times \begin{pmatrix} 0 \\ 0 \\ B \end{pmatrix} = \\ = -eB\begin{pmatrix} v_y(t) \\ -v_x(t) \\ 0 \end{pmatrix} \tag{17}$$

then

$$C(t_1, t_2) = \left(\frac{m}{Ze}\right)^2 \frac{d\mathbf{v}(t_1)}{dt_1}\frac{d\mathbf{v}(t_2)}{dt_2} + \\ + \frac{B^2}{4Z^2}\sum_{i=x,y} v_i(t_1)v_i(t_2) + \frac{mB}{2eZ^2} \times \\ \times \left(\frac{d\mathbf{v}(t_1)}{dt_1}\begin{pmatrix} -v_y(t_2) \\ v_x(t_2) \\ 0 \end{pmatrix} + \frac{d\mathbf{v}(t_2)}{dt_2}\begin{pmatrix} -v_y(t_1) \\ v_x(t_1) \\ 0 \end{pmatrix}\right) = \\ = \left(\frac{m}{Ze}\right)^2 \frac{d\mathbf{v}(t_1)}{dt_1}\frac{d\mathbf{v}(t_2)}{dt_2} + \\ + \frac{5B^2}{4Z^2}\left[v_y(t_1)v_y(t_2) + v_x(t_1)v_x(t_2)\right]. \tag{18}$$

Then the amplitude of the collision operator becomes

$$\phi_{\text{int}} = \phi_1 + \phi_2, \tag{19}$$

where

$$\phi_1 = \frac{2\pi}{3}N_e\left(\frac{\hbar}{em}\right)^2 \int \rho d\rho \int vf(\mathbf{v})d\mathbf{v}\int\limits_{t_-}^{t_+}\int\limits_{t_-}^{t_+} dt_1 dt_2 \times \\ \times \left\{\left(\frac{m}{Ze}\right)^2 \frac{d\mathbf{v}(t_1)}{dt_1}\frac{d\mathbf{v}(t_2)}{dt_2}\right\} \tag{20}$$

and

$$\phi_2 = \frac{2\pi}{3}N_e\left(\frac{\hbar}{em}\right)^2 \int \rho d\rho \int vf(\mathbf{v})db f v\int\limits_{t_-}^{t_+}\int\limits_{t_-}^{t_+} dt_1 dt_2 \times \\ \times \left\{\frac{5B^2}{4Z^2}\left[v_y(t_1)v_y(t_2) + v_x(t_1)v_x(t_2)\right]\right\}. \tag{21}$$

Let first compute ϕ_1. It is easy to write

$$\phi_1 = \left(\frac{m}{Ze}\right)^2 \frac{2\pi}{3} N_e \left(\frac{\hbar}{em}\right)^2 \left(\frac{m}{2\pi KT}\right)^{3/2} \times$$

$$\times \int v\, dv_x dv_y dv_z \exp\left(-\frac{m}{2KT}(v_x^2 + v_y^2 + v_z^2)\right) \times$$

$$\times \int \rho d\rho \int dt_1 \frac{d\mathbf{v}(t_1)}{dt_1} \int dt_2 \frac{d\mathbf{v}(t_2)}{dt_2} =$$

$$= \left(\frac{m}{Ze}\right)^2 \frac{2\pi}{3} N_e \left(\frac{\hbar}{em}\right)^2 \left(\frac{m}{2\pi KT}\right)^{3/2} \times$$

$$\times \int dv_x dv_y dv_z \sqrt{v_0^2 + v_z^2} \exp\left(-\frac{m(v_x^2 + v_y^2 + v_z^2)}{2KT}\right) \times$$

$$\times \int \rho d\rho \int dt_1 \frac{d\mathbf{v}(t_1)}{dt_1} \int dt_2 \frac{d\mathbf{v}(t_2)}{dt_2}, \qquad (22)$$

$$\phi_1 = \left(\frac{m}{Ze}\right)^2 (2\pi)^2 \frac{N_e}{3} \left(\frac{\hbar}{em}\right)^2 \left(\frac{m}{2\pi KT}\right)^{3/2} \times$$

$$\times \int dv_0 dv_z v_0 \sqrt{v_0^2 + v_z^2} \exp\left(-\frac{m(v_0^2 + v_z^2)}{2KT}\right) \times$$

$$\times \int \rho d\rho \int dt_1 \frac{d\mathbf{v}(t_1)}{dt} \int dt_2 \frac{d\mathbf{v}(t_2)}{dt_2} =$$

$$= \left(\frac{m}{Ze}\right)^2 (2\pi)^2 \frac{N_e}{3} \left(\frac{\hbar}{em}\right)^2 \left(\frac{m}{2\pi KT}\right)^{3/2} \times$$

$$\times \int dv_0 dv_z v_0 \sqrt{v_0^2 + v_z^2} \exp\left(-\frac{m(v_0^2 + v_z^2)}{2KT}\right) \times$$

$$\times \int \rho d\rho \left[\mathbf{v}(t_+) - \mathbf{v}(t_-)\right]\left[\mathbf{v}(t_+) - \mathbf{v}(t_-)\right] \qquad (23)$$

such that $t_- \leq t_i \leq t_+$ [26] and

$$t_- = -\frac{\sqrt{R_{\max}^2 - (\rho - r_L)^2}}{|v_z|} \qquad (24)$$

$$t_+ = \tau + \frac{\sqrt{R_{\max}^2 - (\rho - r_L)^2}}{|v_z|} \qquad (25)$$

and

$$v_x = \dot{x} = v_0 \cos(\Omega t), \qquad (26)$$

$$v_y = \dot{y} = v_0 \sin(\Omega t), \qquad (27)$$

$$v_z = v_{0z}. \qquad (28)$$

We calculated the product $\left[\mathbf{v}(t_+) - \mathbf{v}(t_-)\right] \times \left[\mathbf{v}(t_+) - \mathbf{v}(t_-)\right]$. It is also easy to show that

$$\left[\mathbf{v}(t_+) - \mathbf{v}(t_-)\right]\left[\mathbf{v}(t_+) - \mathbf{v}(t_-)\right] =$$

$$= 2v_0^2 \left[1 - \cos\Omega\left(\tau + 2\frac{\sqrt{R_{\max}^2 - (\rho - r_L)^2}}{|v_z|}\right)\right]. \qquad (29)$$

Finally, we get

$$\phi_1 = \left(\frac{m}{Ze}\right)^2 * 2(2\pi)^2 \frac{N_e}{3} \left(\frac{\hbar}{em}\right)^2 \left(\frac{m}{2\pi KT}\right)^{3/2} \times$$

$$\times \int dv_0 dv_z v_0^3 \sqrt{v_0^2 + v_z^2} \exp\left(-\frac{m(v_0^2 + v_z^2)}{2KT}\right) \times$$

$$\times \int \rho d\rho \left[1 - \cos\left(\tau + 2\frac{\sqrt{R_{\max}^2 - (\rho - r_L)^2}}{|v_z|}\right)\right]. \qquad (30)$$

Following the same steps as for ϕ_1, it is easy to find

$$\phi_2 = \left(\frac{5B^2}{4Z^2}\right) \frac{2}{\Omega^2} (2\pi)^2 \frac{N_e}{3} \left(\frac{\hbar}{em}\right)^2 \left(\frac{m}{2\pi KT}\right)^{3/2} \times$$

$$\times \int dv_0 dv_z v_0^3 \sqrt{v_0^2 + v_z^2} \exp\left(-\frac{m(v_0^2 + v_z^2)}{2KT}\right) \times$$

$$\times \int \rho d\rho \int_{t_-}^{t_+} \int_{t_-}^{t_+} \left(\sum_{i=x,y} v_i(t_1) v_i(t_2)\right) dt_1 dt_2 =$$

$$= \left(\frac{5B^2}{4Z^2}\right) \frac{2(2\pi)^2}{\Omega^2} \frac{N_e}{3} \left(\frac{\hbar}{em}\right)^2 \left(\frac{m}{2\pi KT}\right)^{3/2} \times$$

$$\times \int dv_0 dv_z v_0^3 \sqrt{v_0^2 + v_z^2} \exp\left(-\frac{m(v_0^2 + v_z^2)}{2KT}\right) \times$$

$$\times \int \rho d\rho \left[1 - \cos\Omega\left(\tau + 2\frac{\sqrt{R_{\max}^2 - (\rho - r_L)^2}}{|v_z|}\right)\right] \qquad (31)$$

and the complete form of the amplitude of the collision operator in the presence of a magnetic field is summerised in the following expression ($\phi_{\mathrm{int}} = \phi_1 + \phi_2$):

$$\phi_{\mathrm{int}} = \left(\left(\frac{m}{Ze}\right)^2 + \left(\frac{5B^2}{4Z^2}\right) \frac{1}{\Omega^2}\right) 2(2\pi)^2 \frac{N_e}{3} \left(\frac{\hbar}{em}\right)^2 \times$$

$$\times \left(\frac{m}{2\pi KT}\right)^{3/2} \int v_0^3 \sqrt{v_0^2 + v_z^2} \times$$

$$\times \exp\left(-\frac{m}{2KT}(v_0^2 + v_z^2)\right) dv_0 dv_z \times$$

$$\times \int \rho d\rho \left[1 - \cos\left(\tau + 2\frac{\sqrt{R_{\max}^2 - (\rho - r_L)^2}}{|v_z|}\right)\right]. \qquad (32)$$

The first factor can be simplified as:

$$\left(\left(\frac{m}{Ze}\right)^2 + \left(\frac{5B^2}{4Z^2}\right)\frac{1}{\Omega^2}\right) =$$
$$= \frac{1}{Z^2}\left(\left(\frac{m}{e}\right)^2 + \frac{5B^2}{4(\frac{eB}{m})^2}\right) = \frac{9}{4}\left(\frac{m}{Ze}\right)^2. \tag{33}$$

Now, we can write

$$\phi_{int} = \frac{2}{3}\left(\frac{9}{4Z^2}\right)N_e\left(\frac{h}{e^2}\right)^2\left(\frac{m}{2\pi KT}\right)^{3/2} \times$$
$$\times \int dv_0 dv_z v_0^3 \sqrt{v_0^2 + v_z^2}\exp\left(-\frac{m(v_0^2 + v_z^2)}{2KT}\right) \times$$
$$\times \int_{\rho_-}^{\rho_+} \rho\, d\rho\left[1 - \cos\Omega\left(\tau + 2\frac{\sqrt{R_{max}^2 - (\rho - r_L)^2}}{|v_z|}\right)\right], \tag{34}$$

and

$$\begin{aligned}\rho_- &= \max(0, r_L - R_{max}),\\ \rho_+ &= r_L + R_{max}\end{aligned}. \tag{35}$$

Here, $\Omega = eB/m_e$ and $r_L = v_0/\Omega$ are the Larmor frequency and radius, respectively. If we assume $\rho_- = = r_L - R_{max}$ [26] and put the change $y = (\rho - - r_L)/R_{max}$, the amplitude of the collision operator becomes

$$\phi_{int} = \frac{2}{3}\frac{9}{4Z^2}N_e\left(\frac{h}{e^2}\right)^2\left(\frac{m}{2\pi KT}\right)^{3/2}R_{max} \times$$
$$\times \int_{-\infty}^{+\infty} dv_z \int_0^{\infty} v_0^3 \sqrt{v_0^2 + v_z^2}\exp\left(-\frac{m}{2KT}(v_0^2 + v_z^2)\right)dv_0 \times$$
$$\times \int_{-1}^{1}(R_{max}y + r_L)\,dy \times$$
$$\times \left[1 - \cos\Omega\left(\tau + 2R_{max}\frac{\sqrt{1-y^2}}{|v_z|}\right)\right] \tag{36}$$

or, after managing the last integral and replacing Larmor radius r_L by its expression (the term containing R_{max} vanishes, because the integral of an odd function vanishes),

$$\phi_{int} = \frac{N_e}{3}\frac{9}{4Z^2}\left(\frac{2h}{e^2}\right)^2\left(\frac{m}{2\pi KT}\right)^{3/2}\frac{R_{max}}{\Omega} \times$$

$$\times \int_{-\infty}^{+\infty} dv_z \int_0^{\infty} v_0^4 \sqrt{v_0^2 + v_z^2}\exp\left(-\frac{m}{2KT}(v_0^2 + v_z^2)\right)dv_0 \times$$
$$\times \int_0^1 dy\left[1 - \cos\Omega\left(\tau + 2R_{max}\frac{\sqrt{1-y^2}}{|v_z|}\right)\right]. \tag{37}$$

To perform the above integrals, we must to fix the parameters $\tau = \frac{5}{\omega_p}, R_{max} = \frac{5}{2}\lambda_D$ and make changes the velocities

$$\sqrt{\frac{m}{2KT}}\,v_0 = V_0, \tag{38}$$
$$\sqrt{\frac{m}{2KT}}\,v_z = V_Z \tag{39}$$

to get a more suitable expression for the amplitude of the collision operator

$$\phi_{int} = \frac{9}{12Z^2}(J1 + J2 + J3), \tag{40}$$

where we have defined ($U(-\frac{1}{2}, -2, z^2)$ is the Kummer function)

$$J1 = 2A(1 - \cos(\widetilde{F})) \times$$
$$\times 3\frac{\sqrt{\pi}}{8}\int_0^{\infty} dz\exp(-z^2)U\left(-\frac{1}{2}, -2, z^2\right) =$$
$$= 2A(1 - \cos(\widetilde{F})) \times 3\frac{\sqrt{\pi}}{8}\frac{15\pi}{32} =$$
$$= 1.9576A\left(1 - \cos(\widetilde{F})\right) \tag{41}$$

and

$$J2 = \frac{3}{8}\pi\sqrt{\pi}A\widetilde{F}C\cos(\widetilde{F}) \times$$
$$\times \frac{1}{4}G_{2,5}^{3,1}\left(\left(\frac{\widetilde{F}C}{2}\right)^2 \Bigg\| \begin{matrix}\frac{1}{2}, \frac{5}{2}\\ 0, \frac{1}{2}, 3, -1, 0\end{matrix}\right), \tag{42}$$
$$J3 = \frac{3}{8}\pi\sqrt{\pi}A\widetilde{F}C\sin(\widetilde{F}) \times$$
$$\times \frac{1}{4}G_{2,5}^{3,1}\left(\left(\frac{\widetilde{F}C}{2}\right)^2 \Bigg\| \begin{matrix}\frac{1}{2}, \frac{5}{2}\\ 0, \frac{1}{2}, 3, -1, 0\end{matrix}\right), \tag{43}$$

where $G_{2,5}^{3,1}(...)$ is the Meijer function and $A, \widetilde{F}, C$ are defined as

$$A = 40\sqrt{\pi}\frac{m\lambda_D N_e}{eB}\left(\frac{\hbar}{e^2}\right)^2\left(\frac{2KT}{m}\right)^2, \tag{44}$$

$$F = \frac{5eB}{m\omega_p} = 5\frac{\Omega}{\omega_p}, \tag{45}$$

$$C = \omega_p \lambda_D \sqrt{\frac{m}{2KT}}, \quad \widetilde{F} = 2\pi F. \tag{46}$$

Finally, the collision operator in the presence of a magnetic field reads

$$\phi_{\text{int}} = \frac{15Q}{4\widetilde{F}C}\left(1 - \cos(\widetilde{F})\right) + Q(\cos(\widetilde{F}) + \sin(\widetilde{F})) \times$$

$$\times G_{2,5}^{3,1}\left(\left(\frac{\widetilde{F}C}{2}\right)^2 \middle| \begin{array}{c} \frac{1}{2}, \frac{5}{2} \\ 0, \frac{1}{2}, 3, -1, 0 \end{array}\right). \tag{47}$$

The direct collision operator amplitude $\phi_d = \frac{\phi_{\text{int}}}{2}$,

$$\phi_d = \frac{15Q}{8\widetilde{F}C}\left(1 - \cos(\widetilde{F})\right) + \frac{Q}{2}(\cos(\widetilde{F}) + \sin(\widetilde{F})) \times$$

$$\times G_{2,5}^{3,1}\left(\left(\frac{\widetilde{F}C}{2}\right)^2 \middle| \begin{array}{c} \frac{1}{2}, \frac{5}{2} \\ 0, \frac{1}{2}, 3, -1, 0 \end{array}\right), \tag{48}$$

is such that

$$Q = \frac{9\pi\sqrt{\pi}}{128}\frac{A\widetilde{F}C}{Z^2}, \tag{49}$$

with

$$\widetilde{F} = 9.7902 \times 10^7 \frac{B(\text{Tesla})}{\sqrt{N_e(\text{cm}^{-3})}}, \tag{50}$$

$$\widetilde{F}C = 6.9227 \times 10^7 * \frac{B(\text{Tesla})}{\sqrt{N_e(\text{cm}^{-3})}}, \tag{51}$$

$$A\widetilde{F}C = 3.7198 \times 10^5 * T^{\frac{5}{2}}. \tag{52}$$

3. Results and Discussion

We have calculated the collision operator numerically using expressions (47)–(52) for hydrogen-like ions for various plasma parameters to show the variation of this operator. First, we can see clearly from these expressions that the collision operator variation with a magnetic field is related to the combination of four functions $\frac{1}{B}$, $\cos(B)$, $\sin(B)$, and the Meijer function. We present now the variation of ϕ_B as a function of the magnetic field B for $B = 100$ to $10\,000$ T at $T = 100$ eV and at densities $N_e = 10^{22}$ cm^{-3} for hydrogen-like Ag^{+46} and hydrogen-like Ar^{+17} in Figs. 1 and 2. It is seen that the variation of the collision operator as a function of the magnetic field has
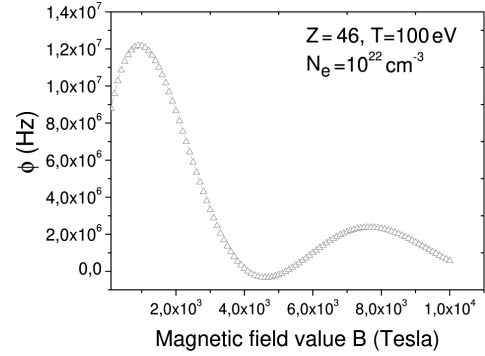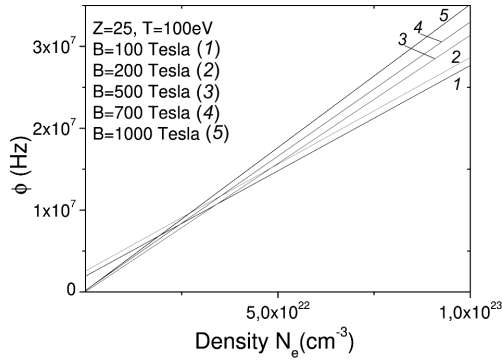

Fig. 1. The amplitude of the collision operator versus the magnetic field B for Silver hydrogen-like (Ag^{+46})
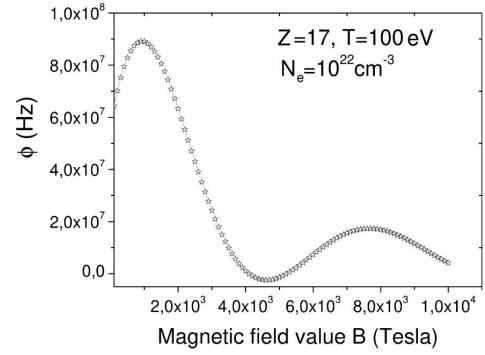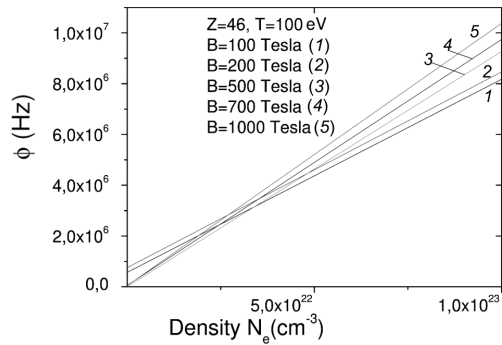

Fig. 2. The amplitude of the collision operator versus the magnetic field B for Argon hydrogen-like (Ar^{+17})

a sinusoidal shape enveloped by an increasing amplitude which returns to $\left(\frac{1}{B}\right)$ function. We can explain it by the fact that the electron has a helical trajectory. Therefore, at increasing the value of the magnetic field, the electron moves away from the emitter ion, and the collisions become less strong. We can note the same takes place for Ar^{+17} (Fig. 2). As a function of the density, in the range of 10^{18} cm^{-3} to 10^{26} cm^{-3}, we have plotted the collision operator amplitude ϕ_B at the 100-eV temperature and for 100 T to $1\,000$ T. Figure 3 for hydrogen-like Fe^{+25} shows that, with increasing the density, the collision operator amplitude ϕ_B decrease, but always remains very large for the strong field. The same remarks can be made for Ag^{+46}, but with less amplitudes (see Fig. 4).
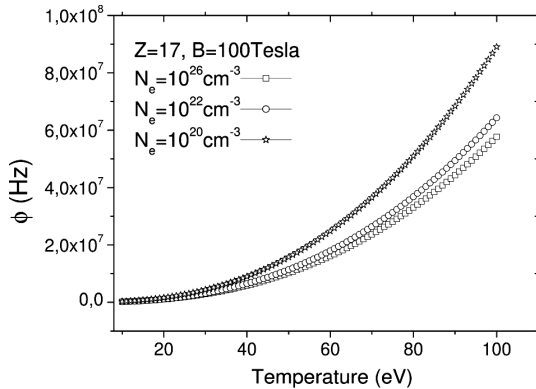
In Fig. 5, we give the collision operator amplitude ϕ_B versus the temperature and for different densities of hydrogen-like Ar^{+17} for $B = 100$ T. We can see that this variation is a function as $T^{5/2}$, so, in a very hot plasma, the amplitude of the collision

Fig. 3. The amplitude of the collision operator versus the density for different magnetic fields B for Iron hydrogen-like (Fe^{+25})


Fig. 4. The amplitude of the collision operator versus the density for different magnetic fields B for Silver hydrogen-like (Ag^{+46})

**Fig. 5.** The amplitude of the collision operator for Argon hydrogen-like (Ar^{+17}) versus the temperature for the magnetic field $B = 100$ T for different densities

operator increases with the temperature. This is expected, because, in the extra hot plasma, the electrons become more in motion, and, therefore, the col-
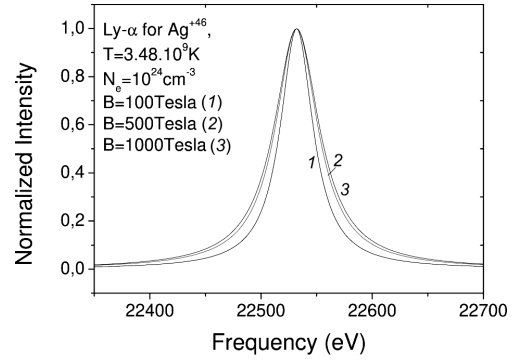
Fig. 6. The line profile of Lyman-alpha for Silver hydrogen-like (Ag^{+46}) plotted for three magnetic fields
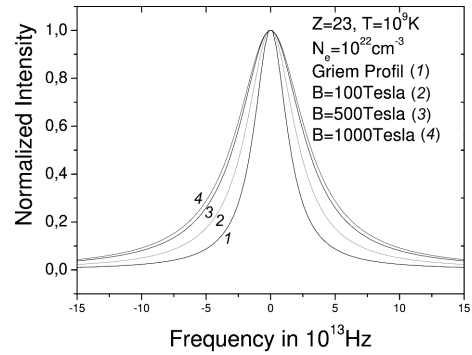
Fig. 7. The line profile of Lyman-alpha for Vanadium hydrogen-like (Vn^{+22}) plotted for three magnetic fields

Table 1. **The FWHM broadened by free electrons for three magnetic field values (100, 500, and 1,000 T) and by Doppler effect in eV for the temperature $T_e = 3.48 \times 10^9$ K and the density $N_e = 10^{26}$ cm^{-3}: the first line corresponds to CrXXIV and the second to FeXXVI, and the experimental width is from Ref. [28], whereas $\Delta\omega_c$ is from [9]**

$\Delta\omega_{\text{exp}}$, eV Shot Z1141	$\Delta\omega_D$, eV without B	$\Delta\omega_C$, eV without B	B	our $\Delta\omega$, eV	our $\Delta\omega +$ $+ \Delta\omega_D$
Cr^{+23} 50	Cr^{+23} 34.375	Cr^{+23} 15.52	100 500 1000	17.2218 17.3276 17.4118	51.597 51.703 51.787
Fe^{+25} 65	Fe^{+25} 39.2	Fe^{+25} 11.16	100 500 1000	12.5582 12.6199 12.6967	51.758 51.820 51.897

lisions increase. We have also calculated the Lyman-α line of hydrogen-like ions without fine structure at $T = 100$ eV and $N_e = 10^{22}$ cm^{-3} for different values

of magnetic field B. We have just included the broadening by electron collisions, as well as the Doppler broadening.

Figure 6 shows the line profile of hydrogen-like Ag^{+46} including only the collision broadening just to check the influence of the magnetic field. We see that, with increasing the magnetic field B, the line profile becomes more broadened.

To make our work more valid, we have compared our results with some published researches: in Table, we presented the FWHM (Full Width at Half Maximum) broadened by free electrons for three magnetic field values and by the Doppler effect in eV unit's for the temperature $T_e = 3.48 \times 10^9$ K and the density $N_e = 10^{26}$ cm^{-3}: the first line corresponds to CrXXIV and the second to FeXXVI, and the experimental width $\Delta\omega_{\exp}$ is from Ref. [28], while the classical width is from Ref. [9]. In fact, the paper by Haines (2006) [28] is devoted to the measurement of the electron and ion temperatures for a magnetically confined plasma, by using the K-shell emission lines. In the experience, they considered some Z pinches (Z1137 and Z1141), as example, shot Z1141 on the Z accelerator at Sandia, which employed a 450 g = cm nested stainless-steel wire array with an initial outer array diameter of 55 mm, inner one of 27.5 mm and a 2:1 mass ratio. The measured electron temperature from line ratios and the continuum slope is found to be 3 keV at stagnation. In addition to the dominating Cr and Fe lines, Mn and Ni ones are apparent. The agreement was again quite good, well within the error associated with that of the measurement.

It is clair that the Doppler broadening is dominant. However, in the presence of a magnetic field, our results become more important than the classical width, when the magnetic field increase, and approaches the experimental values.Therefore, we can confirm that our results are in good agreement with experiment.

In another side, we have plotted the spectral line shape of hydrogen-like V^{+22} at $T = 10^9$ K and the densities about $N_e = 10^{22}$ cm^{-3} studied in work [29], we note that only the electronic broadening is included here. Figure 7 shows the comparison between the line broadened by electronic collisions in no-magnetized plasma (Griem profile) and magnetied plasma for different magnetic field values. It is clear that, in magnetized plasma, the line becomes more broadened, as compared to Griem profile. With in-

creasing the magnetic field, the line becomes more and more broadened.

4. Conclusion

The various broadening mechanisms in magnetized plasmas increase the complexity of the analysis of line shapes. However, the complexity provides the possibility that an accurate model of the perturbed emitter may lead to more information on the plasma conditions. In this work, we have traited and calculated the operator of electronic collisions in the presence of a magnetic field. Our model allows us to analyze the collision operator, as well as the spectra of different emitters for a wide range of plasma conditions. For hot and dense plasma at laboratories under the conditions of thermonuclear fusion, in some stars, and in astrophysical plasmas (tokamaks, e.g.) for very strong field values, the collision operator amplitude calculations show a signifcant effect. We have studied the Lyman-α line for some emitters such as hydrogen-like V^{+22}, Ag^{+46}, Cr^{+23}, and Fe^{+25}, neglecting the ionic Stark broadening, the comparaison with experience and with another researches gives a good agreement. So, in magnetized plasma, the collisions become more important, and the line profile becomes more broadened.

1. A. Naam, M. Meftah, S. Douis *et al.* Spectral line broadening by relativistic electrons in plasmas: Collision operator. *Advances in Space Research* **54**, 1242 (2014).
2. Sandrine Ferri, Annette Calisti, Caroline MossпïS *et al.* Ion dynamics effect on stark-broadened line shapes: A cross-comparison of various models. *Atoms* **2** (3), 299 (2014).
3. A. Calisti, C. MossпïS, S. Ferri *et al.* Dynamic Stark broadening as the Dicke narrowing effect. *Phys. Rev. E* **81**, 016406 (2010).
4. A. General, U. Shpenik. Modeling of gas discharge in water vapor. *Ukr. J. Phys.* **58**, 116 (2013).
5. M. Baranger. Simplified quantum-mechanical theory of pressure broadening. *Phys. Rev.* **111**, 481 (1958).
6. M. Baranger. Problem of overlapping lines in the theory of pressure broadening. *Phys. Rev.* **111**, 494 (1958)

7. S. Alexiou. Collision operator for isolated ion lines in the standard Stark-broadening theory with applications to the *Z* scaling in the Li isoelectronic series 3P-3S transition. *Phys. Rev. A* **49**, 106 (1994).

8. E. Sadeghzadeh Lari, H. Askari, M. Meftah *et al.* Calculation of electron density and temperature of plasmas by using new Stark broadening formula of helium lines. *High Energy Density Physics* **26**, 68 (2018).

9. K. Arif, M.T. Meftah, K. Chenini *et al.* Contribution of LiïnïSnard? Wiechert potential to the broadening of spectral lines by electron collisions. *Phys. Plasmas* **29**, 093303 (2022).

10. P. Zeeman. The effect of magnetisation on the nature of light emitted by a substance. *Nature* **55**, 347 (1897).

11. S. Ferri, O. Peyrusse, A. Calisti. Stark–Zeeman line-shape model for multi-electron radiators in hot dense plasmas subjected to large magnetic fields. *Matter Radiat. Extremes* **7**, 015901 (2022).

12. A. Raji, R. Rosato, J. Stamm *et al.* New analysis of Balmer line shapes in magnetic white dwarf atmospheres. *Eur. Phys. J. D* **75**, 1 (2021).

13. E. Oks. Influence of magnetic-field-caused modifications of trajectories of plasma electrons on spectral line shapes: Applications to magnetic fusion and white dwarfs? *J. Quant. Spectrosc. Radiat. Transf.* **171**, 15 (2016).

14. E. Oks. Corrigendum to: ?Influence of magnetic-field-caused modifications of trajectories of plasma electrons on spectral line shapes: Applications to magnetic fusion and white dwarfs? *J. Quant. Spectrosc. Radiat. Transf.* **175**, 107 (2016).

15. Ny Kieu, JoñïSl Rosato, Roland Stamm *et al.* A new analysis of stark and zeeman effects on hydrogen lines in magnetized da white dwarfs. *Atoms* **5**, 44 (2017).

16. S.O. Kepler, I. Pelisoli, S. Jordan *et al.* Magnetic white dwarf stars in the sloan digital sky survey. *Mon. Not. R. Astron. Soc.* **429**, 2934 (2013).

17. J.D. Landstreet, S. Bagnulo, G.G. Valyavin *et al.* On the incidence of weak magnetic fields in DA white dwarfs. *Astron. Astrophys.* **545**, 1 (2012).

18. J. Rosato, N. Kieu, I. Hannachi *et al.* Stark–Zeeman line shape modeling for magnetic white dwarf and tokamak edge plasmas: Common challenges. *Atoms* **5** (4), 36 (2017).

19. R. Brauer, S. Wolf, S. Reissl, F. Ober. Magnetic fields in molecular clouds: Limitations of the analysis of Zeeman observations. *Astron. Astrophys.* **601**, 1 (2017).

20. L. Godbert-Mouret, M. Koubitia, R. Stamm *et al.* Spectroscopy of magnetized plasmas. *Q. R. S. T.* **71**, 365 (2001).

21. E. Stambulchik, Y. Maron. Zeeman effect induced by intense laser light. *Phys. Rev. Lett. E* **113**, 083002 (2014).

22. S. Fadhel, M.T. Meftah, K. Chenini. Quantum dynamics of hydrogen-like ions in a spatially nonuniform magnetic field: A possible application to fusion plasma. *Atoms* **6**, 1 (2022).

23. O. Loginov, O. Cheremnykh, V. Krivodubskij *et al.* Kinematic dynamo model of a solar magnetic cycle. *Ukr. J. Phys.* **67**, 796 (2022).

24. S. Nasrin, M. Bose. Effect of two different electron temperatures in auroral ionosphere. *Ukr. J. Phys.* **67**, 136 (2022).

25. J. Rosato, S. Ferri, R. Stamm. Influence of helical trajectories of perturbers on Stark Line shapes in magnetized plasmas. *Atoms* **6** (1), 12 (2018).

26. S. Alexiou. Line shapes in a magnetic field: Trajectory modifications I: Electrons. *Atoms* **7** (2), 52 (2019).

27. S. Alexiou. Line Shapes in a magnetic field: Trajectory modifictions II: Full collision-time statistics. *Atoms* **7** (4), 94 (2019).

28. M.G. Haines, P.D. LePell, C.A. Coverdale *et al.* Ion viscous heating in a magnetohydrodynamically unstable *Z* pinch at over 2×10^9 Kelvin. *Phys. Rev. Lett.* **96**, 075003 (2006).

29. D. Zenkhri, M. Meftah, F. Khelfaoui. Relativistic calculation of spectral line broadening by electron collisions in plasmas: Case of hydrogenic ions. *Advances in Space Research* **69**, 3553 (2022).

Х. Герріда, К. Ченіні, М.Т. Мефтах,
С. Дуіз, Д.Е. Зенхрі, К. Аріф

ОПЕРАТОР ЗІТКНЕНЬ
ДЛЯ НЕЗВ'ЯЗАНИХ ЕЛЕКТРОНІВ
У МОДЕЛІ НАМАГНІЧЕНОЇ ПЛАЗМИ

Форми спектральних ліній плазми містять інформацію щодо параметрів плазми і можуть бути використані для її діагностики. Отримано формулу з функцією Мейєра для оператора зіткнень електронів плазми в зовнішньому магнітному полі. В рамках деякого наближення розглядається взаємодія між випромінюючими системами (воднеподібними йонами) та електронами плазми. Розраховано амплітуду оператора зіткнень йонів Ar^{+17}, V^{+22}, Cr^{+23}, Fe^{+25} та Ag^{+46} в інтервалі густин 10^{18}–10^{26} см$^{-3}$ при температурах 10^6–10^{10} К в дуже сильному магнітному полі 100–10 000 Т. Результати для Лайман-альфа лінії добре узгоджуються з експериментальними даними та іншими теоретичними результатами.

К л ю ч о в і с л о в а: оператор зіткнень для електронів, зовнішнє магнітне поле, спектроскопія плазми.